UNIVERSIDAD NACIONAL DE COLOMBIA
SEDE MEDELLÍN
FACULTAD DE MINAS

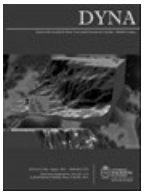

DYNA
http://dyna.medellin.unal.edu.co/

Carbon nitride films grown by cathodic vacuum arc for hemocompatibility applications

Diana Shirley Galeano-Osorio [a], Santiago Vargas [a], Rogelio Ospina-Ospina [b], Elisabeth Restrepo-Parra [b] & Pedro José Arango [b]

[a] *Facultad de Minas, Universidad Nacional de Colombia. dsgaleanoo@unal.edu.co*
[b] *Facultad de Ciencias Exactas y Naturales, Laboratorio de Física del Plasma Universidad Nacional de Colombia. erestrepopa@unal.edu.co*

Received: July 30th, de 2013. Received in revised form: March 27th, 2014. Accepted: April 21th, 2014

Abstract

Amorphous carbon nitride films have been obtained by pulsed cathodic arc at substrate temperatures of 20, 100, 150 and 200 °C. Film structure was investigated by Fourier Transformed infrared spectroscopy (FTIR) and Raman spectroscopy. Nitrile bands at approximately 2200 cm^{-1} were identified in all films. As the temperature increased a reduction in the concentration of sp^3 bonds and a decrease in the structure disorder were observed. The relative intensity ratio of Raman D and G bands increased as the substrate temperature increased from 20 to 100°C. Nevertheless, at a critical temperature of 150°C, this trend was broken, and the film became amorphous. A peak at approximately 1610 cm^{-1} of films grown at 100°C, 150°C and 200 °C suggests that CNx is dominated by a relatively ordered graphite ring like glassy carbon. Moreover, the film grown at 150 °C presented the lowest roughness and the highest hardness and hemocompatibility.

Keywords: Carbon nitride films; Raman spectroscopy; FTIR spectroscopy; substrate temperature.

Películas de nitruro de carbono crecidas por arco catódico en vacío para aplicaciones en hemocompatibilidad

Resumen

Se obtuvieron películas delgadas de nitruro de carbono amorfo empleando arco pulsado y variando la temperatura del sustrato a temperatura ambiente, 100, 150 y 200 °C. Los enlaces de las estructuras se investigaron empleando la técnica de espectroscopía infrarroja por transformada de Fourier (FTIR) y espectroscopía Raman. Se identificaron bandas de nitrilos en aproximadamente 2200 cm^{-1}. Se observó una reducción en la concentración de los enlaces sp^3 y del desorden estructural de las películas. La relación entre las intensidades de las bandas D y G aumentó con la temperatura del sustrato desde temperatura ambiente hasta 100°C; sin embargo, a una temperatura crítica de 150°C, esta tendencia desapareció y las películas se tornaron amorfas. Se observó un pico ubicado en aproximadamente 1610 cm^{-1} en las películas crecidas a 100°C, 150°C y 200 °C; además, las películas crecidas a 150 °C presentaron la rugosidad más baja y mayores durezas y hemocompatibilidad.

Palabras clave: Películas de nitruro de carbono; Espectroscopía Raman; Espectroscopía FTIR; Temperatura del sustrato.

1. Introduction

Surface coating is an effective method to improve the durability of materials used in aggressive environments [1-3]. The search for hard materials has pointed to carbon nitride films because investigations have predicted that the hardness of the β-C3N4 structure is high, even comparable to that reported for diamond [4]. In fact, studies of this hard structure have been extended to amorphous carbon nitride films. Amorphous carbon nitride coatings exhibit optimal biocompatibility [5], electronic [6] and mechanical properties [7]; therefore, these films are very attractive for many applications. Several deposition methods have been used to prepare carbon nitride (a-C:N) films, such as sputtering and arc deposition [8,9], among others. Using continuous or pulsed arc discharges, a-C:N films are easy to grow because arc discharges are an efficient way to ionize nitrogen gas to produce free N+ such that nitrides can be easily formed. One problem commonly faced when producing films by vacuum arc discharge is the generation of nanoparticles. Hakovirta et al. [10] carried out a study on carbon-based thin films with a pulsed vacuum arc system with and without particle filtering. In their final remarks, the researchers concluded that

the surface of the coatings produced with the unfiltered system is quite rough, but in many applications, the original surface of the sample is even rougher. Moreover, the high production rate and simplicity of the system without filtering relative to the characteristics of the filtered system are great advantages. On the other hand, substrate temperature, T_S, is recognized as a key parameter influencing the composition of CN_x films and also the bonds within such films [11]; several investigations have shown that high substrate temperatures encourage the formation of a crystalline phase, whereas low temperatures could cause amorphous structures to develop in the films. The results obtained by Chen et al. indicated that higher substrate temperatures could promote the formation of a C_3N_4 phase [12]. Fuge et al. observed that CN_x films deposited at low T_S are amorphous, and CN_x films grown at higher T_S tend to be increasingly nanocrystalline [11]. In general, some properties such as stress and roughness were found to be strongly dependent on the deposition temperature, changing the film structure (sp^2 and sp^3 bonds) above a certain transition temperature. This critical temperature normally depends on the deposition system. For instance, Zhou et al. [13,14] produced CNx coatings by the vacuum cathodic arc method varying the substrate temperature. They found that at 200°C, the films properties changed drastically. One of the main goals of this study was to find the most suitable deposition conditions, particularly the optimal substrate temperature, for producing CN_x coatings with the highest sp^3/sp^2 bond ratio, keeping in mind further applications of these films as hard coatings or biocompatible coatings. To this end, the coating structures were analyzed as a function of substrate temperature. Spectroscopic characterization techniques such as Fourier transform infrared spectroscopy and Raman scattering can provide valuable information about the structural properties [15].

Thus, the aim of the present paper is to report the growth of a-CN_x films prepared by the unfiltered pulsed vacuum cathodic arc technique. Moreover, studies on the effects of substrate temperature on the structure of carbon nitride thin films were conducted. Spectroscopic techniques were used to characterize chemical bonds and the modifications to the films' microstructure.

2. Experimental setup

The experimental setup is presented in Fig. 1. The equipment used to produce the coatings was a non-commercial reaction chamber made of stainless steel.

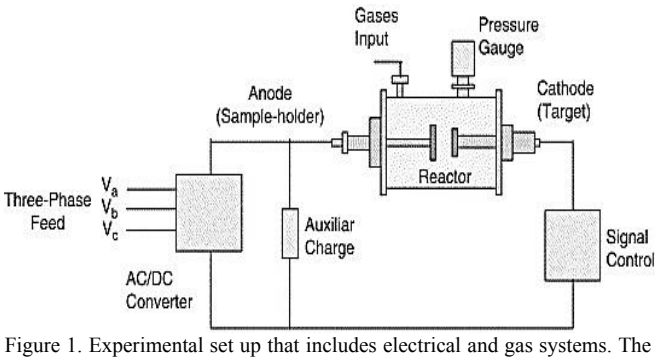

Figure 1. Experimental set up that includes electrical and gas systems. The reaction chamber contains the electrodes (anode and cathode).
Source: The authors

Double-sided electrodes were placed in this chamber. A high-power supply designed to generate pulses with different active and passive times was used to produce an arc discharge between the electrodes. The inter-electrode pulsed voltage can be varied from 0 to 280 Vrms (root mean square voltage) with a 150 A maximum working current, depending on the experiment. In this case the work voltage used was 240 V_{rms}. The active time is limited by the minimum necessary value for arc ignition under given working conditions, such as target material, working gas and pressure. The inactive arc time can take any theoretical value; nevertheless, it is necessary to take into account that the minimum value is subjected to the arc extinction time under the given working conditions (mainly the target material and the working gas) [16]. The heating system was placed inside the anode to make it possible to heat the substrate in-situ. Carbon nitride films were produced using a graphite target of 99.999% purity that measured 2.00 cm in diameter and 0.250 mm in thickness. The deposition conditions were as follows: four arcs, 1 s active time, 2 s inactive time, 11.7 mm distance between electrodes. Nitrogen was used as the working gas at a pressure of 260 Pa. The substrates were 316L stainless steel disks that measured 2 mm in thickness and 12.7 mm in diameter. These substrates were previously polished using sandpaper with grit sizes ranging from 60 to 1500. Finally, acetone was used to eliminate impurities. Additionally, a KCl crystal measuring 2 mm in thickness and 12.7 in mm diameter was used as the substrate where coatings were grown to carry out the FTIR analysis.

The substrate holder (anode) was heated by a resistance coil below the holder. During the deposition, the substrate temperature was maintained at RT, 100 °C, 150 °C and 200 °C. This range of temperature was chosen according to a previous work reported by our group, where at values close to these, coatings presented a good performance [17]. After deposition, a vacuum pressure up to approximately 10^{-2} Pa was reached, allowing the sample to cool until reaching room temperature. The system is well described in previous works [16].

IR transmission measurements were performed using a Perkin Elmer BXII FTIR spectrometer over the wave number range 400-4000 cm^{-1}. A 4-cm^{-1} spectral resolution was used for all measurements under normal conditions. Raman scattering measurements were carried out using the 473-nm line of a DPSS laser operating at 5.5 mW in the 900–1900-cm^{-1} region with a LabRam HR800 Horiba Jobin Yvon instrument. The spectra were deconvoluted with the Grams 32 program.

For structural characterization, scanning probe microscopy (SPM) was used in the atomic force microscopy (AFM) mode. For this characterization, a Park Scientific Instruments Autoprobe CP with probes made of silicon and ProScan image-processing software were used. To obtain topographic images of the films in AFM mode, a cantilever probe of silicon nitride (Si_3N_4) with a spring constant of 0.16 N/m was used under environmental conditions with a scanning speed of 1 Hz and image resolution of 256×256 pixels. The measurements were taken at 60% relative humidity and 24 °C. These analyses were performed by capturing five images from different sites on each coating and averaging them. The films' hardness was also obtained with the SPM equipment. Small forces (applied over distances on the order of nanometers) with a precision of 0.2 nN were used.

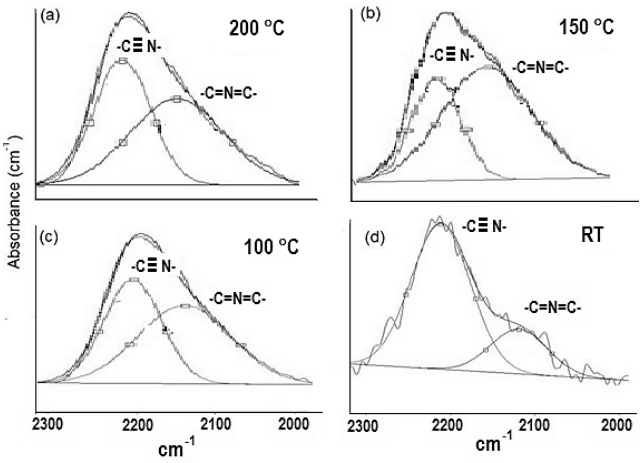

Figure 2. 2300-2000-cm^{-1} region fit of CN_x films' FTIR spectra: a) 200 °C, b) 150 °C, c) 100 °C and d) RT.
Source: The authors

Platelet-adhesion in vitro tests were performed on the CNx films obtained at various TS. Blood was taken from a healthy adult and collected in sodium citrate as an anticoagulant. First, the blood was centrifuged for 6 min at 5500 rpm, and approximately 1 ml of lighter substances was separated from the blood plasma. Then, the remaining material was centrifuged again for 5 min at 2400 rpm, allowing for the extraction of the platelet-rich plasma (PRP). Samples were immersed in the PRP and incubated at 37°C for 120 min; afterward, the samples were rinsed with a 0.9% NaCl solution to remove weakly adherent platelets and then fixed in 2% glutaraldehyde.

Environmental scanning electron microscopy (ESEM) was used to study the quantity and morphology of the adherent platelets, after which the films' thrombogenicity was evaluated. Photographs of the platelets were taken randomly and the thrombogenicity results were correlated with the films' roughness and microstructure.

3. Results and Discussion

3.1. FTIR Analysis

In Fig. 2, the FTIR spectra show bands between 2000 and 2300 cm^{-1}. These bands were curve-fitted, and two Gaussian contributions were found. The results obtained are summarized in Table 1.

$$\frac{sp^3}{sp^2} = \frac{Log\left(\frac{I_0}{I}\right)_{sp^3}}{Log\left(\frac{I_0}{I}\right)_{sp^2}} \quad (1)$$

High-energy contributions attributed to nitrile terminal groups -C≡N [18] and low-energy vibration modes involving terminal groups such as carbodiimides, -N=C=N- [19] can be seen. In addition, the low-energy vibrations also induce a stretching phase located in the spectral range between 1460 and 1500 cm^{-1} [20]. In order to calculate the relative concentration of sp^3, sp^2 and sp^1 bonds from FTIR spectra, the next equation is employed.

Table 1
FTIR energy bands of CNx films at various substrate temperatures.

FTIR bands	Figure	Energy-band position (cm^{-1})			
		RT	100 °C	150 °C	200 °C
C≡N	Fig. 2	2211±8	2204±6	2210±4	2203±9
-N=C=N-		2118±5	2163±4	2172±5	2167±8
C=N	Fig. 3	1626±7	1618±7	1609±8	1584±4
Phenyls or -N=C=N-		1422±4	1448±5	1505±9	1432±7
C-C		1406±6	1407±8	1407±6	1408±5
C-N		1139±5	1187±7	1200±6	1252±8
C-N or C-O					1051±6

Source: The authors

For this method Io is approximately obtained drawing a straight line between the points of lower transmission placed at each side of the maximum, and I is the intensity of the maximum [21].

Table 2 presents the relative concentration of sp2 (C=N) and sp1 (C≡N) bonds as the sp2/sp1 ratio. At low temperatures, sp1 bonds prevail over sp2(sp2/sp1<1) because the total energy of the structure after a single N substitution for sp2 formation is, on average, 1 eV higher than that for sp1 formation [22]; nevertheless, this tendency ceases at TS=150 °C, possibly because TS provides sufficient energy for sp2 formation, producing an increase in the sp2/sp1 ratio; however, at 200 °C, the sp2/sp1 ratio decreases again because the adatoms mobility increased.

A great part of the energy is expended in moving the adatoms and not in forming sp2 bonds. The spectral region between 1850 and 850 cm-1 reveals C-C, C=C, C-N and C=N bond contributions. Fig. 3 shows the spectra for this region with varying TS. A Gaussian deconvolution with a linear background was carried out in this region, and the energy-band positions are listed in Table 1. Several spectral

Table 2
Relative concentration ratios sp^2/sp^1 and $sp^3/sp^2$for CN*x* films at various substrate temperatures.

Bonds ratio (adim.)	Energy-band ratio (adim.)			
	RT	100 °C	150 °C	200 °C
(sp^2/sp^1) $C_{C=N}/C_{C\equiv N}$	0.33 ±0.05	0.22 ±0.04	1.15 ±0.09	0.25 ±0.02
(sp^3/sp^2) $C_{C-N}/C_{C=N}$	0.86 ±0.05	0.94 ±0.04	1.76 ±0.10	1.11 ±0.08
C/N From XPS	0.18 ±0.02	0.25 ±0.08	0.3 ±0.06	0.27 ±0.09
(sp^2/sp^1) $C_{C=N}/C_{C\equiv N}$	0.33 ±0.05	0.22 ±0.04	1.15 ±0.09	0.25 ±0.02
(sp^3/sp^2) $C_{C-N}/C_{C=N}$	0.86 ±0.05	0.94 ±0.04	1.76 ±0.10	1.11 ±0.08
C/N From XPS	0.18 ±0.02	0.25 ±0.08	0.3 ±0.06	0.27 ±0.09

Source: The authors

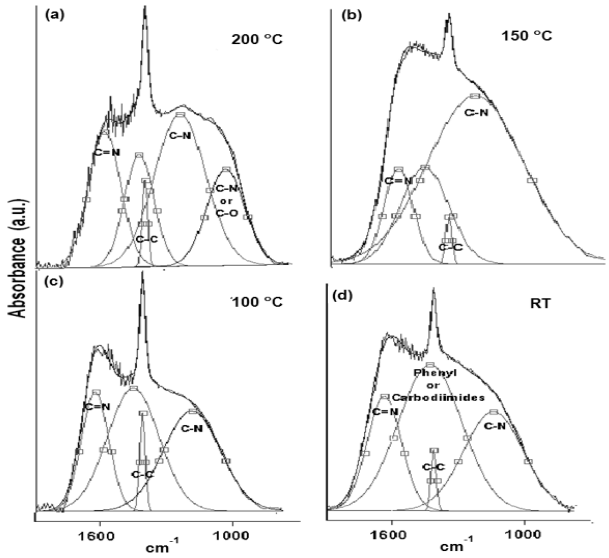

Figure 3. 1850-800-cm-1 region fit of FTIR spectra: a) 200 °C, b) 150 °C, c) 100 °C and d) RT.
Source: The authors

differences depending on TS can be highlighted. At RT, 100 °C and 150 °C, a well-defined fit can be achieved using four Gaussian contributions. Nevertheless, for the sample grown at 200 °C, one more peak is added to attain a suitable deconvolution. The bands ranging between 1650 and 1600 cm-1 have been attributed to C=N stretching [23]. According to Hammer et al., these configurations are bonded mainly to the aromatic cluster edges [23]. They may also be associated with pyridine vibrational modes, with bands around 1620-1560 cm^{-1} [24].

The decrease in the energy as the temperature increases is attributed to changes in the films' microstructure caused by the heating process. The band at approximately 1407 cm-1 may have been produced by sp3 C-C [25]. The bands ranging from 1300 to 1139 cm-1 are reported to be due to C-N simple bonds [26]. An increase in the vibrational energy as Ts increased was observed. These results are consistent with an increase in the degree of ordering of the C-N clusters [27]. For films grown at 200 °C, the band located at approximately 1050 cm-1 could be attributed to C-N vibrations [16] or C-O stretching, which can be found in the range between approximately 1160 and 1080 cm-1 [28].

Table 3
Raman parameters and intensity ratio of different satellite components for the *a*-CN*x*films at various substrate temperatures.

Band	Energy-band position (cm^{-1})			
	RT	100 °C	150 °C	200 °C
G	1560±1	1563±1	1571±1	1583±3
D	1359±8	1357±6	1362±7	1374±2
N	1412±3	1398±4	1396±7	1398±6
C=C	1603±1	1610±1	1611±1	1612±2
	Band broadening (cm^{-1})			
D	100.8±0.6	100.5±0.4	96.6±0.3	91.7±0.2
G	86.2±0.5	98.3±0.3	127.0±0.5	83.8±0.3
	Band ratio (adim.)			
I_D/I_G	0.37±0.04	0.54±0.05	1.4±0.4	1.6±0.3
I_N/I_G	3.9±0.4	4.3±0.2	6±0.4	5.3±0.3

Source: The authors

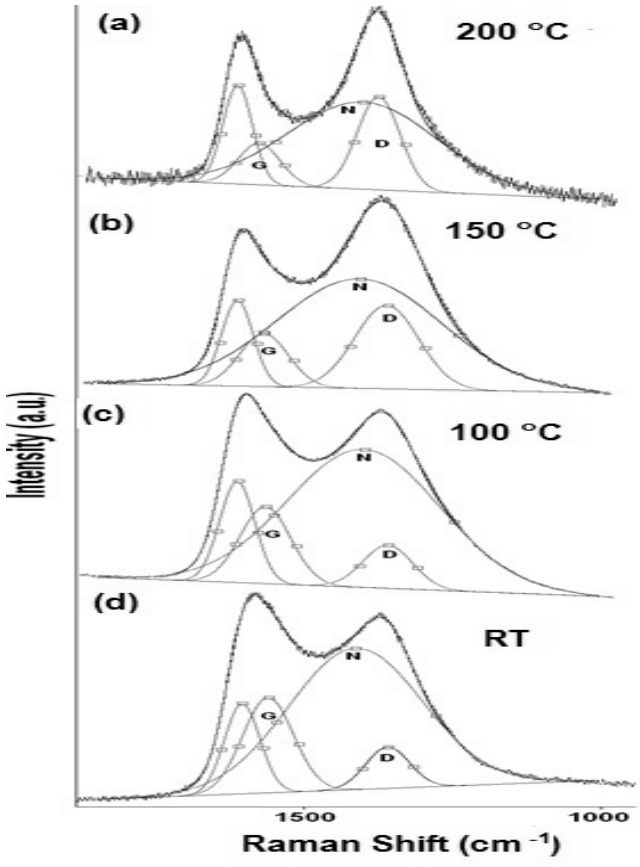

Figure 4. D and G band fit Raman spectra: a) 200 °C, b) 150 °C, c) 100 °C and d) RT.
Source: The authors

Moreover, an analysis of the relative concentration of sp3 (C-N) and sp2 (C=N) bonds in the films as a function of TS was carried out. These values are shown in Table 2. In this table, an increase in the concentration of sp3 C-N bonds in the case of the film grown at 150 °C was observed. At this temperature, aromatic amines and C-N bonds are formed, which are more thermodynamically favorable. This increase could explain the shift of the phenyl radical toward high energies with respect to the phenyl species in the other films.

3.2. Raman Analysis

Fig. 4 shows the Raman spectra of the CNx films with varying TS. Gaussian deconvolution with a linear background for frequencies between 1000 and 1850 cm-1 was carried out. To attain a better fit, four bands were employed. The positions of the D (disorder) and G (graphite) bands, their broadening and their intensity ratio ID/IG for each film are summarized in Table 3. The increase in the ID/IG ratio as the temperature increases suggests graphitization by heating, including an increase in disorder in the ring angles and lengths. Because the shift in the G band toward higher frequencies is accompanied by an increase in the ID/IG ratio. There may have been an increase in the size or number of sp2 domains. This shift is

only observed when six-fold aromatic rings are present [29]. The shift in the D toward higher frequencies suggests the densification of the sp2 ringed structure in the lattices. The increase in the ID/IG ratio, widening of the D-peak and narrowing of the G-peak are caused by increase of the graphite-like component in the amorphous carbon films [30]. Capelli [31] demonstrated that higher I_D/I_G ratio and narrower G are associated to the carbon configuration changes from an amorphous mixture of sp^3/sp^2 configuration to a locally ordered sp^2 nano-graphite structure. The widening of the D band is related to the presence of more sp^2 carbon bond angle distortion [32]. This behavior increases the disorder and decrease the graphite-like structure in the crystalline region of the film.

The N peak is visualized between the D and G bands as shown in Fig. 4. This peak is due to N=N stretching vibrations when N is bonded to a carbon ring, particularly one of the C-N=N-C benzene type [33]. The N=N stretching frequencies vary between 1400 and 1500 cm^{-1} depending on the site replaced by carbon. This is also correlated with the degree of symmetry breaking [34]. An increase in the I_N/I_G area ratio was observed as a function of the substrate temperature, as is shown in Table 2. The N incorporation in films grown at RT, 100°C and 200°C could benefit the formation of aromatic clusters. Nevertheless, the increase in the nitrogen content of the films produced at 150°C could favor the formation of pyridine rings, which blocks cluster growth. Furthermore, an increase in the number of -C≡N nitrile bonds may occur at 150°C because as terminal groups, they prevent the growth of graphitic clusters. This assertion is supported by the relative concentration ratio $C_{C\equiv N}/C_{C=N}$ shown in Table 2. The increase in the number of N=N bonds may indicate that the films contain large amounts of nitrogen, implying that as the substrate temperature rises, the nitrogen concentration increases. The substrate temperature favors the atomic surface migration of C and N species, accelerating chemical reactions between different species and increasing the nitrogen concentration [35]. The nitrogen concentration decreases again at 200 °C. This behavior can be attributed to the fact the C and N species can be desorbed at this T_S. The subsequent drop in nitrogen content at 200°C, as shown in Table 1, may be due to an increase in the desorption of some volatile species, such as C_2N_2 and nitriles [35]. Moreover, higher substrate temperatures are unfavorable for the incorporation of more-volatile species such as CN [36]. The transition to a more crystalline phase as the substrate temperature increases may be caused by a relaxation process in the film structure provoked by the heating treatment. This relaxation may also be related to the desorption of N species observed in this film because the desorption of N atoms from the rings can cause C atoms to take their place, thereby stabilizing and relaxing the structure. Each spectrum contains a peak beyond1600 cm^{-1}. This finding may be related to the D peak of glassy carbon, which corresponds to C=C stretching in aromatic rings [37], indicating that the films have a higher tendency toward graphitization. The increase in the T_S caused the frequencies to shift toward higher values due to changes in the films' microstructure because of the heat treatment. Fig. 5 shows the XPS C1s spectra of the CNx film grown at TS=150 °C, presenting several components. This spectrum was decomposed into three components fitted with Gaussian functions by approximating the background contribution using Shirley's method.

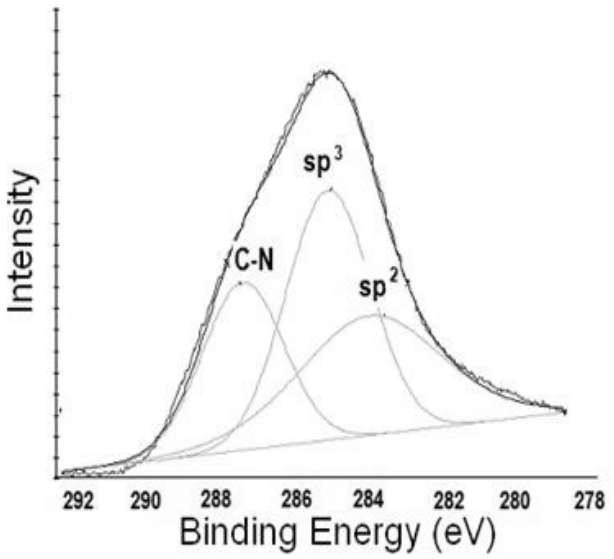

Figure 5. XPS spectrum of the C 1s peak obtained for the coating produced at room temperature.
Source: The authors

The first component peaked at 284.6 eV corresponds to sp^2 carbon bonds, the second one at 285.5 eV is related to sp^3 carbon bonds and the fourth component at 287.5 eV comes from C–N bonds [38]. This result corroborates the presence of carbon linked nitrogen. N/C atomic percentage depending on T_S was included in Table 2. Similar to Raman spectroscopy results, the nitrogen percentage increases as the substrate temperature rises.

3.3. AFM Analysis

AFM images were obtained for various T_S, as shown in Fig. 6. Irregular surfaces with poor uniformity and agglomerations were observed. The film thicknesses remained within the same order of magnitude (approximately 450 nm). According to Figs. 6 (a) and (c), the films grown at RT and 100 °C presented small grain sizes, in the order of 300 nm, compared with the films produced at 150 °C and 200 °C that exhibit values of around 800 nm, as is shown in Figs 6(e) and (g). Although CNx-coating morphologies characterized by small grains have been reported by several authors [39], the coatings produced in this work exhibited different behavior because the films' morphology depends on many factors, such as the growth parameters and technique and the chemical composition.

The roughness and thickness of films grown at different T_S were measured and are listed in Table 4. Films grown at RT, 100 °C and 200 °C presented high roughness and low thickness, in agreement with values reported by other researchers [36].

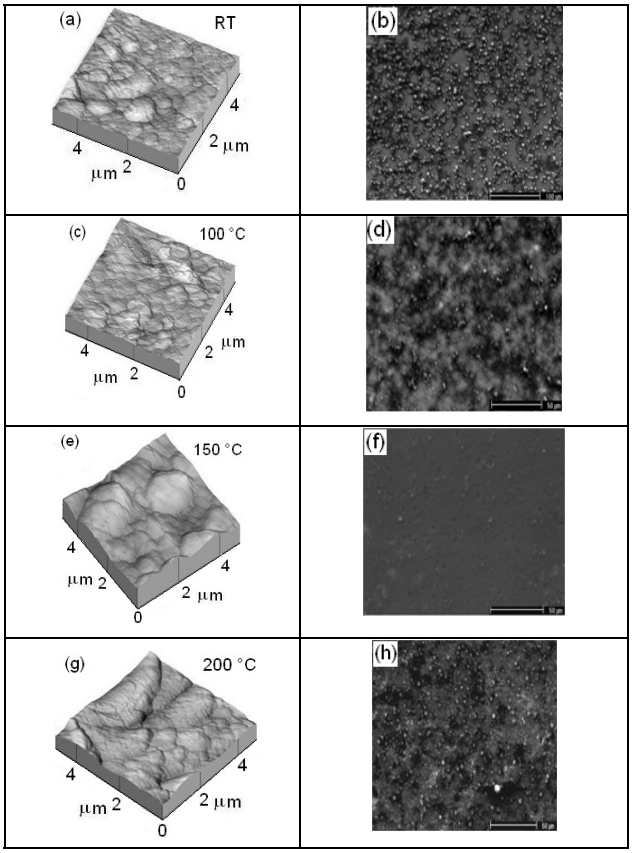

Figure 6. Surface images of the CNx films grown at different temperatures (left) and SEM micrographs of films after thrombogenicity analysis (right). Source: The authors

Table 4
Roughness thickness and hardness of CNx films grown at various T_S

T_S (°C)	Roughness (nm)	Thickness (nm)	Hardness (GPa)
RT	55.98±3.0	378±8	10.5±2.1
100	61.22±2.6	457±7	10.4±1.1
150	11±1	638±10	13.5±3.0
200	51.33±9.7	557±8	6.0±1.0

Source: The authors

Studies carried out by A. Stanishevsky regarding the morphology of CNx films deposited at different pressures revealed non-uniform surfaces due to large graphitic domains and a CN polymeric component. A large polymeric component results in low roughness, whereas a greater number of graphitic clusters induce the formation of more or larger agglomerations [40].

3.4. Hardness

On the other hand, there is a relationship between the chemical composition and the nano-hardness of the films. The results presented in Table 4 show that the film grown at 150 °C exhibited the highest hardness and the highest sp^3/sp^2 bond ratio.

According to the literature, the hardness of carbon-based films is determined by the existence of sp^3-hybridized C bonds. The highest hardness, which was exhibited by the film grown at 150 °C, can be explained by the disorder induced by the sp^3 bonds between the aromatic layers. These bonds can exist if the distance between the layers is shorter than the interplanar distance of graphite, as dictated by van der Waals interactions. These bonds produce structure densification, compaction and ultimately greater hardness [41].

3.5. ESEM Analysis

Platelet adhesion on the CNx films obtained at various T_S was analyzed by the ESEM technique, as shown in Figs. 6 (b), (d), (f) and (h). On films grown at RT, 100 °C and 200 °C, the platelets showed a high degree of spreading and attained activation. They linked together and formed aggregations. However, the coating obtained at 150 °C showed poor platelet adherence. Moreover, on this coating, the platelets remained inactivated, without exhibiting pseudopodia, and they remained almost isolated. The hemocompatibility was observed to improve as the films tended toward graphitization, as shown for the film grown at 150°C (the highest I_D/I_G ratio and nitrogen concentration). High N content delays clotting and defers platelet activation. This film was the most blood-compatible, presenting the fewest adherent blood platelets and lowest level of platelet aggregation [42]. Among the plasma proteins, fibrinogen is regarded as the key protein that triggers platelet adhesion, activation and aggregation. Subsequently, coagulation factors are released, initiating the coagulation cascade and the eventual formation of a thrombus. In addition, the hemoglobin, platelet and a few plasma proteins in blood tend to be negatively charged. Usually the material surface with more unsaturated bonds in electronegativity has better thromboresistance according to the principle of same electric charge mutual repulsion. In the case of CNx coatings, they include $sp^2C\backslash N$ and $sp^3C\backslash N$ bonds at the surface and polarize the surface due to the difference in electronegativity between carbon and nitrogen [43].

4. Conclusions

The CNx films were obtained with the pulsed cathodic vacuum arc method at several substrate temperature. FTIR spectroscopy analysis indicated the formation of carbon-nitrogen bonds with sp^3, sp^2 and sp^1 hybridization. The results obtained from Raman spectroscopy suggest that the deposited amorphous carbon nitride films have a graphitic structure. However, at the critical substrate temperature, 150°C, the structure became more amorphous, perhaps due to the increase in the N concentration inside the lattice. At 150 °C, films exhibited the highest hardness and the highest sp^3/sp^2 bond ratio.

The hemocompatibility was observed to improve as the films tended toward graphitization, as shown for the film grown at 150°C. This film was the most blood-compatible, showing the fewest adherent blood platelets and lowest level of platelet aggregation.

Acknowledgments

The authors gratefully acknowledge the financial support of the División para la Investigación de la Universidad Nacional de Colombia Sede Manizales (DIMA).

References

[1] Ruden, A., González Carmona, J.M., Restrepo, J.S., Cano, M.F. and Sequeda, F., Tribología de recubrimientos de ZrN, CrN y TiAlN obtenidos por magnetron sputtering reactivo, DYNA, 80 (178), pp. 95-100, 2013.

[2] Muñoz, J.E. and Coronado J.J. Análisis mecánico y tribológico de los recubrimientos Fe-Cr-Ni-C y Ni-Al-Mo, DYNA, 74 (153), pp. 111-118, 2007.

[3] Copete H., López, E., Vargas Galvis F., Echavarría A. and Ríos T., Evaluación del comportamiento in vitro de recubrimientos de hidroxiapatita depositados mediante proyección térmica por combustión oxiacetilénica sobre un sustrato de Ti6Al4V, DYNA 80 (177), 101-107, 2013.

[4] Liu, A.Y. and Cohen, M.L., Prediction of new low compressibility solids, Science, 245 (4920), pp. 841-842, 1989. DOI:10.1126/science.245.4920.841

[5] Wei, S., Shao, T. and Ding, P., Study of CNx films on 316L stainless steel for orthodontic application, Diamond. and Related Materials, 19 (5-6), pp. 648-653, 2010.

[6] Cappelli, E., Trucchi, D.M, Kaciulis, S., Orlando S., Zanza, A. and Mezzi A., Effect of deposition temperature on chemical composition and electronic properties of amorphous carbon nitride (a-CNx) thin films grown by plasma assisted pulsed laser deposition, Thin Solid Films, 519, pp. 4059-4063, 2011.

[7] Zhang, K., Wen, M., Meng, Q.N., Zeng, Y., Hu C.Q., Liu C. and Zheng W.T., Structure, mechanical property, and tribological behavior of c-NbN/CNx multilayers grown by magnetron sputtering, Surface and Coatings Technology, 206, pp. 4040-4045, 2012.

[8] Mishra, S.K., Shekhar, Ch. and Rupa, P.K.P. and Pathak, L.C., Effect of pressure and substrate temperature on the deposition of nano-structured silicon–carbon–nitride superhard coatings by magnetron sputtering, Thin Solid Films, 515, pp. 4738-4744, 2007.

[9] Hsieh, W.-J., Shih, P.-S., Lin, Ch.-Ch., Wang, Ch.-Y. and Shih H.C., Structure and optical property of the a-C:N films synthesized by filtered cathode vacuum arc, Surface Coating Technology, 200, pp. 3175-3178, 2006.

[10] Hakovirta, M., Salo, J., Lappalainen, R. and Antitila A., Correlation of carbon ion energy with sp^2/sp^3 ratio in amorphous diamond films produced with a mass-separated ion beam, Physics Letter A, 205 (49), pp. 287-289, 1995.

[11] Fuge, G. M., Rennick, Ch.J., Pearce, S.R.J., May, P.W., Ashfold, M.N.R., Structural characterisation of CNx thin films deposited by pulsed laser ablation, Diamond Related Materials, 12, pp. 1049-1054, 2003.

[12] Chen, Z.Y., Zhao, J.P., Yano T., Ooie, T., and Sakakibara, M.J., Effect of temperature on carbon nitride films synthesized by ion-beam-assisted pulsed laser deposition, Journal of Applied Physics, 88, pp. 7060-7066, 2000.

[13] Zhou Z., Xia L. and Sun M., Carbon nitride films prepared at various substrate temperatures by vacuum cathodic arc method, Diamond Related Material, 13 (1). pp. 14-21, 2004.

[14] Zhou Z., Xia L., Sun M., The investigation of carbon nitride films deposited at various substrate temperatures and N2/Ar flow ratios by vacuum cathodic arc method, Applied Surface Science, vol. 222 (14-), pp. 327-337, 2004.

[15] Lejeune, M., Durand-Drouhin, O., Charvet, S., Zeinert, A. and Benlahsen, M., On the induced microstructure changes of the amorphous carbon nitride films during annealing, Journal of Applied Physics, 101 (12), pp. 123501, 2007.

[16] Ospina R., Castillo, H.A., Benavides, V., Restrepo, E., Arango, Y.C., Arias, D.F. and Devia, A., Influence of the annealing temperature on a crystal phase of W/WC bilayers grown by pulsed arc discharge, Vacuum, 81 (3), pp. 373-377, 2006.

[17] Ospina R., Escobar D., Restrepo-Parra, E. Arango, P.J. and Jurado, J.F., Substrate temperature influence on W/WCNx bilayers grown by pulsed vacuum arc discharge, Applied Surface Science, 258 (12), pp. 5100-5104, 2012.

[18] Chalmers, J.M., Griffiths, P.R., Eds. Handbook of vibrational spectroscopy, Vol. 1, Theory and Instrumentation, John Wiley & Sons, Inc., 2003

[19] Lejeune, M., Charvet, S., Zeinert, A. and Benlahsen, M., Optical behavior of reactive sputtered carbon nitride films during annealing, Journal Applied Physics, 103 (1), pp. 013507, 2008.

[20] Bouchet-Fabre B., Marino, E., Lazar, G., Zellama, K., Clin, M., Ballutaud, D., Abel, F. and Godet C., Spectroscopic study using FTIR, Raman, XPS and NEXAFS of carbon nitride thin films deposited by RF magnetron sputtering, Thin Solid Films, 482 (1-2), pp. 167-171, 2005.

[21] Segura-Giraldo, B., Restrepo-Parra, E. and Arango-Arango P.J., On the influence of a TiN interlayer on DLC coatings produced by pulsed vacuum arc discharge: Compositional and morphological study, Applied Surface Science, vol. 256 (1), pp. 136-141, 2009.

[22] Bouchet-Fabre, B., Fernandez, V., Gohier, A., Parent, P., Laffon, C., Angleraud, B., Tessier, P.Y. and Minea, T.M., Temperature effect on the nitrogen insertion in carbon nitride films deposited by ECR, Diamond Related Materials, 18 (9), pp. 1091-1097, 2009.

[23] Hammer, P., Baker, M.A., Lenardi, C. and Gissler, W., Synthesis of carbon nitride films at low temperatures, Journal of Vacuum Science Technology A, 15 (1), pp. 107-112, 1997.

[24] Zhao, X.-A., Ong, C.W., Tsang, Y.C., Chan, K.F., Choy, C., Chan, P.W. and Kwok, R.W.M., Relationship between the structure and the optical and electrical properties of ion beam deposited CNx films, Thin Solid Films, 322 81-2), pp. 245-253, 1998.

[25] Zhang J., Liu, W., Li, X., Zhan, B., Cui, Q. and Zou, G., Well-crystallized nitrogen-rich graphitic carbon nitride nanocrystallites prepared via solvothermal route at low temperature, Materials Research Bulleting, 44, pp. 294, 2009.

[26] Li, Z., Zhou, J., Zhang, J., Chen, T. and Yuan, J., Carbon nitrides synthesized by glow discharge method, Journal of Alloys and Compounds, 346 (1-2), pp. 230-234, 2002.

[27] Lazar, G., Clin, M., Charvet, S., Therasse, M., Godet, C. and Zellama, K., Effect of the RF power and deposition temperature on the electrical and vibrational properties of carbon nitride films, Diamond Related Materials, 12 (2), pp. 201-207, 2003.

[28] Majumdar, A., Schäfer, J., Mishra, P., Ghose, D., Meichsner J., and Hippler R., Chemical composition and bond structure of carbon-nitride films deposited by CH_4/N_2 dielectric barrier discharge, Surface and Coatings Technology, 201, pp. 6437-6444, 2007.

[29] Kovács, G., Veres, M., Koós, M. and Radnóczi, G. Raman spectroscopic study of magnetron sputtered carbon-nickel and carbon nitride-nickel composite films: the effect of nickel on the atomic structure of the C/CNx matrix, Thin Solid Films, 516, pp. 7910-7915, 2008.

[30] Wang, J., Huang, N., Pan, C.J., Kwok, S.C.H., Yang, P., Leng, Y.X., Chen, J.Y., Sun, H., Wan, G.J., Liu, Z.Y. and Chu, P.K., Bacterial

repellence from polyethylene terephthalate surface modified by acetylene plasma immersion ion implantation–deposition, Surface and Coatings Technology, 186 (1-2), pp. 299-304, 2004.

[31] Cappelli, E., Scilletta, C., Orlando, S., Valentini, V. and Servidori, M., Laser annealing of amorphous carbon films, Applied Surface Science, 255, pp. 5620-5625, 2009.

[32] Marcinauskas, L., Grigonis, A., Valatkevicius, P. and Medvid, A. Irradiation of the graphite-like carbon films by ns-laser pulse, Applied Surface Science, 261, pp. 488-492, 2012.

[33] Colthup, N.B., Daly, L.H. and Wiberly, S.E., Introduction to infrared and raman spectroscopy, 3rd Ed., Academic Press, New York, 1990.

[34] Chowdhury, A., Cameron, D. and Hashmi, M., Vibrational properties of carbon nitride films by Raman spectroscopy, Thin Solid Films, 332 (1-2), pp. 62-68, 1998.

[35] Wang, X., Li, Z., Wu, P., Jiang, E. and Bai, H., Annealing effects on the microstructure of amorphous carbon nitride films, Applied Surface Science, 253 (4), pp. 2087-2092, 2006.

[36] Sebald, T., Kaltofen, R. and Weise, G. Reactively r.f. magnetron sputtered carbon nitride films, Surface and Coatings Technology, 98 (1-3), pp. 1280-1285, 1998.

[37] McCulloch, D., Prawer, S. and Hoffman, A., Structural investigation of xenon-ion-beam-irradiated glassy carbon, Physical Review B, 50, pp. 5905-5917, 1994.

[38] Khun, N.W. and Liu, E., Effect of substrate temperature on corrosion performance of nitrogen doped amorphous carbon thin films in NaCl solution, Thin Solid Films, 517 (17), pp. 4762-4767, 2009.

[39] Zemek, J., M. Jelinek, M., Vorlicek, V., Trchova, M., Lancok, J., Carbon nitride layers created by laser deposition combined with RF discharge, Diamond and Related Materials, vol. 9 (3), pp. 548-551, 2000.

[40] Stanishevsky, A., On the surface morphology of C:N films deposited by pulsed cathodic arc discharge method, Materials Letter, 37 (3), pp. 162-167, 1998.

[41] Huang, Z., Yang, B., Liu, C., Guo, L., Fan, X. and Fu, D., Effect of annealing on the composition, structure and mechanical properties of carbon nitride films deposited by middle-frequency magnetron sputtering, Materials Letter, 61 (3), pp. 3443-3445, 2007.

[42] Galeano-Osorio, D.S., Vargas, S., López-Córdoba, L.M., Ospina, R., Restrepo-Parra, E., Arango, P.J., Substrate temperature influence on the trombogenicity in amorphous carbon nitride thin coatings, Applied Surface Science, 256 (24), pp. 7484, 2010.

[43] Zhao, M.L., Li D.J., Guo, M.X., Zhang, Y.T., Gu, H.Q., Deng, X.Y., Wan, R.X., Sun, X., The different N concentrations induced cytocompatibility and hemocompatibility of MWCNTs with CNx coatings, Surface and Coatings Technology, 229, pp. 90-96, 2013.

D. S Galeano-Osorio, received a Bs. Eng in Physical Engineering in 2006, an MSc degree in Physics in 2009, and she is studying for a PhD in Engineering, science and technology of materials since 2011, all of them from the Universidad Nacional de Colombia. Her research interests include: production and characterization of materials by plasma assisted techniques for applications in hemocompatibility.

S. Vargas-Giraldo, received a Bs. Eng in Physical Engineering in 2005. He has worked in several industries in Colombia dedicated to the material processing by plasma assisted techniques. He is an expert in plasma reactors instruments for industrial applications.

R. Ospina-Ospina, received a Bs. Eng in Physical Engineering in 2005, an MSc degree in Physics in 2010, and a PhD degree in Engineering, science and technology of materials in 2011. Currently, he is carrying out his second posdoc in the Centro Brasileiro de Pesquisa Fisica. His research interests include: Materials processing by plasma assisted techniques, materials characterization by SEM, XRD, TEM among others and new materials production.

E. Restrepo-Parra, received a Bs. Eng in Electrical Engineering in 1990 from the Universidad Tecnológica de Pereira, an MSc degree in Physics in 2000, and a PhD degree in Engineering – automation in 2009, the last two from the Universidad Nacional de Colombia, sede Manizales. From 1991 to 1995, she worked in the Colombian electrical sector and since 1996 for the Universidad Nacional de Colombia. Currently, she is a senior Professor in the Physics and Chemistry Department, Facultad de Ciencias Exactas y Naturales, Universidad Nacional de Colombia – sede Manizales. Her research interests include: simulation and modeling of materials properties by several methods; Materials processing by plasma assisted techniques and materials characterization. She is currently Director of Laboratories Sede Manizales, Universidad Nacional de Colombia.

P.J. Arango-Arango, received a Bs. in Physics in 1982, an MSc degree in Physics in 1987, all of them from the Universidad de Valle, Colombia. Currently, he is a full Professor in the Physics and Chemistry Department, Facultad de Ciencias Exactas y Naturales, Universidad Nacional de Colombia – sede Manizales. His research interests include: Materials processing by plasma assisted techniques and materials characterization. He is currently Director of the Laboratorio de Física del Plasma, Universidad Nacional de Colombia.